A methodology to relate octane numbers of binary and ternary n-heptane, iso-octane and toluene mixtures with simulated ignition delay times

A Methodology to Relate Octane Numbers of Binary and Ternary n-heptane, iso-octane and Toluene Mixtures with Simulated Ignition Delay Times

Jihad A. Badra[1*], Nehal Bokhumseen[1], Najood Mulla[1], S. Mani Sarathy[2], Aamir Farooq[2], Gautam Kalghatgi[1], Patrick Gaillard[1]

[1]Saudi Aramco Research and Development Center, Fuel Technology R&D Division, Dhahran 31311, Saudi Arabia

[2]Clean Combustion Research Center, Division of Physical Sciences and Engineering, King Abdullah University of Science and Technology (KAUST), Thuwal 23955, Saudi Arabia

*Corresponding Author –Email: jihad.badra@aramco.com, Phone: +966544636600

Innovation Cluster 3, KAUST, Thuwal, Mekkah province, 23955, Saudi Arabia

Abstract

Predicting octane numbers (ON) of gasoline surrogate mixtures is of significant importance to the optimization and development of internal combustion (IC) engines. Most ON predictive tools utilize blending rules wherein measured octane numbers are fitted using linear or non-linear mixture fractions on a volumetric or molar basis. In this work, the octane numbers of various binary and ternary n-heptane/iso-octane/toluene blends, referred to as toluene primary reference fuel (TPRF) mixtures, are correlated with a fundamental chemical kinetic parameter, specifically, homogeneous gas-phase fuel/air ignition delay time. Ignition delay times for stoichiometric fuel/air mixtures are calculated at various constant volume conditions (835 K and 20 atm, 825 K and 25 atm, 850 K and 50 atm (research octane number RON-like) and 980 K and 45 atm (motor octane number MON-like)), and for variable volume profiles calculated from cooperative fuel research (CFR) engine pressure and temperature simulations. Compression ratio (or ON) dependent variable volume profile ignition delay times are investigated as well. The constant volume RON-like ignition delay times correlation with RON was the best amongst the other studied conditions. The variable volume ignition delay times condition correlates better with MON than the ignition delay times at the other tested conditions. The best correlation is achieved when using compression ratio dependent variable volume profiles to calculate the ignition delay times. Most of the predicted research octane numbers (RON) have uncertainties that are lower than the repeatability and reproducibility limits of the measurements. Motor octane number (MON) correlation generally has larger uncertainties than that of RON.

Keywords: Octane numbers, ignition delay times, toluene primary reference fuels, chemical kinetics.

1. Introduction

As the global energy demand for transportation increases, so does the demand for more efficient automobile vehicles. One of the main concerns and limiting factors in the automotive industry is the engine knock phenomenon [1-3]. Engine knock, according to Morgan et al. [4], can be defined as a "limiting factor of a spark ignition (SI) engine's thermodynamic efficiency caused by the auto-ignition of the fuel/air mixture ahead of the turbulent flame front".

Practical fuels such as gasoline, diesel and jet fuels are complex mixtures of hundreds of different components. The autoignition chemistry of practical fuels is thus very complicated and difficult to predict accurately. Ignition delay time measurement devices, such as shock tubes (ST) and rapid compression machines (RCM), cannot be used to fully understand the knock phenomenon because these idealized reactors operate at near-constant volume reaction conditions. On the other hand, pressure and temperature evolve and cover wide range of conditions in practical devices such as engines. Therefore, fuel anti-knock quality has to be described by empirical measurements, known as Research and Motor Octane Numbers, RON and MON. These tests are run in a single-cylinder CFR (Cooperative Fuels Research) engine in accordance with the procedures set in ASTM D2699 for RON and ASTM D2770 for MON [5]. The RON test is run at an engine speed of 600 rpm and an intake temperature of 52 °C while the MON test is run at 900 rpm and a higher intake temperature of 149 °C.

Since commercial gasoline fuels consist of a range of compounds that are not universally consistent due to the differences in the crude oil origin and refinery processes [6], understanding the fuel behaviour becomes a multifaceted issue. To simplify this problem, it has been proposed that fuel behaviour can be modelled through simple mixtures (surrogates) that mimic the real fuel properties under certain conditions. Iso-octane is the simplest surrogate for gasoline and it is usually used to describe flame propagation [7]. However, the autoignition properties of real gasoline cannot be adequately described by iso-octane because of its high octane numbers (RON = MON = 100). Therefore, Primary Reference Fuels (PRFs), which are mixtures of n-heptane and iso-octane, are used to match the gasoline octane numbers. By definition, PRFs have zero sensitivity, where sensitivity is defined to be the difference of RON and MON (sensitivity = RON-MON). Hence, two different PRFs are needed to match real gasoline octane numbers under RON and MON conditions [8-10]. Real gasoline fuels have sensitivities up to 11 because they contain considerable amounts of branched paraffins, olefins and aromatics. Thus, a sensitive component must be added to PRF blends to match octane numbers and sensitivities of the real gasoline. Aromatics, such as toluene, are generally added to PRF blends to account for the missing sensitivity. Shock tube [11] and engine experiments [12] have demonstrated that blends of n-heptane/isoc-octane/toluene, known as toluene primary reference fuel (TPRF) blends, can adequately represent autoignition behaviour of gasoline [4, 11, 12]. Some researchers have proposed gasoline surrogates that contain more than three compounds. Mehl et al. [13] proposed a four component surrogate comprising n-heptane, iso-octane, toluene and 1-hexene (olefin) to represent the ignition behaviour of RD-387 gasoline. Perez and Boehman [14]

investigated 5 component surrogates where they added methylcylco-hexane (naphthenes) on top of the four components proposed by Mehl et al. [13]. Naik et al. [15] replaced 1-hexene with 1-pentene to formulate their 5 components surrogates similar to [14]. Fikri et al. [16] studied the effect of adding diisobutylene to TPRFs and Yahyaoui et al. [17] investigated mixtures containing iso-octane, toluene, 1-hexene and ethyl-tert-butyl-ether (ETBE). Recently, Sarathy et al. [18] and Ahmed et al. [19] proposed 5 and 6 component surrogates to reproduce the ignition delay characteristics of alkane-rich gasoline fuels.

Significant amount of work has been reported on TPRF surrogates and validated chemical kinetic models exist in literature [13, 16, 20], so this work focuses only on TPRFs. The methodology used to TPRF surrogate composition for a real gasoline is crucial in order to accurately determine the mixture's RON and MON. The most common method of blending the surrogate components (n-heptane, iso-octane, toluene) is through blending rules that are developed based on data fittings from various experimental data sets. Lately, a study conducted by Knop et al. [21] on octane number prediction methods of TPRF fuel mixtures found that the linear-by-mole blending rule produce the best results in terms of accuracy. The results from their proposed blending rule were compared with six different existing methods and previously published experimental data. Recently, Kalghatgi et al. [22] proposed a new non-linear-by-mole blending rule that was based on a wide range of CFR experimental data for TPRF mixtures. Although these methodologies prove to give reasonably accurate results in predicting the ON of TPRF, the addition of any other components, such as ethanol, to the mixture causes the blending rule to fail [14, 23].

Several studies have focused on trying to link the ON from CFR engine to basic chemical kinetic parameters. Leppard [9] related the sensitivity of the fuel to the negative temperature coefficient (NTC) behaviour of various fuels. Curran et al. [24] and Mehl et al. [25] proposed that the ON might actually correlate with the critical compression ratio (CCR). Hori et al. [26, 27] investigated possible relation between ON and ignition properties within micro-flow reactors (MFR). Furthermore, Mehl et al. [13] and Sarathy et al. [28] examined the possibility that ON might correlate with homogeneous gas-phase ignition delay times. Mehl et al. [13] tried to correlate the anti-knock index (AKI=(RON+MON)/2) with ignition delay times of stoichiometric fuel/air mixtures at 825 K and 25 atm, whereas Sarathy et al. [28] chose different conditions (835 K and 20 atm) to relate RON to homogeneous ignition delay times. Both authors utilized constant volume simulations for their correlations, while Sarathy et al. [28] also included experimental shock tube ignition delay data acquired for pure components (normal and branched alkanes) for the correlation.

The purpose of this study is to provide a methodology to associate a fuel's research octane number (RON) and motor octane number (MON) with the homogeneous gas-phase ignition delay times through the use of chemical kinetic simulations. Ignition delay times are calculated at various conditions to investigate possible correlation with ON. Constant volume ignition delay times were tested by using the previously proposed temperature and equivalence ratio conditions of Mehl et al. [13], Sarathy et al. [28] and newly proposed RON-like and MON-

like conditions. Variable pressure and temperature profiles from CFR engine experiments were also tested. Finally, compression ratio and octane number dependent pressure and temperature profiles were investigated, and a promising correlation between ON and ignition delay times was obtained.

2. Prediction Methodology and Numerical Approach

To obtain a correlation between ignition delay times and ON for TPRF fuels, CFR measurements in the literature were collected and used for the current analysis. Recently, our group published a new set of CFR experimental data for TPRF mixtures with the toluene concentration varying from 10% to 90% by volume [22]. For each toluene percentage, iso-octane (vol.%)/n-heptane (vol.%) was varied from 0 to 100. This experimental data set was utilized to develop a new non-linear by mole blending rule, which was validated against other data from literature [22]. In the current work, new CFR measurements were performed so that the prediction can cover a wider range of octane numbers. The newly collected data are primarily for n-heptane/toluene mixtures with varying toluene concentration from 10% to 80% by volume. Also, MON measurements for some TPRF mixtures were not provided in [22] and are measured in the current work. The CFR data from Knop et al. [21], Morgan et al. [4] and ASTM [29, 30] were also utilized here. The new experimental measurements are presented in Table 1. The various data sets from literature used in the current work are presented in Table S1 (Supplementary Material).

CHEMKIN-PRO [31] was used to perform all ignition delay time simulations presented in this work. Simulations were performed for a homogenous batch reactor with constant UV (constrain volume and solve energy equation) assumptions. However, a volume profile was used in the calculations when pressure and temperature profiles are required. Volume profiles were calculated from the measured CFR pressure profiles via isentropic relations. More details on volume profiles calculations are given in the subsequent sections. The detailed gasoline surrogate mechanism developed by Mehl et al. [13, 32] was employed to simulate ignition delay times for the mixtures presented in Table 1 and Table S1. Because the global stoichiometry in the CFR engine is around 1, stoichiometric (Φ=1) TPRF/air mixtures were used in all simulations presented in this work. Please note that all the subsequent correlations are specific to this particular chemical kinetic mechanism. Using different chemistries will result in different correlations if there are differences in calculated ignition delay times.

3. Results and Discussions

3.1. Condition 1: Constant volume ignition delay times at 835 K and 20 atm

Ignition delay times of the fuel/air stoichiometric mixtures presented in Table 1 and Table S1 were calculated at constant volume conditions. First, the conditions (835 K and 20 atm) proposed by Sarathy et al. [28] were investigated. Figure 1a shows the RON and MON as functions of ignition delay times calculated at 835 K and 20

atm (logarithmic scale) for the Kalghatgi et al. [22] and current TPRF blends. As can be seen from Fig. 1a, a correlation exists between ignition delay times and ON for the various TPRF mixtures. However, a scatter can be observed from the plotted data. For example, three mixtures with similar RON values (≈ 66) that have been tested in the same CFR engine ([22] and current) have three different ignition delay times, as illustrated in Table 2 (C1). Also, there is noticeable scatter in the ON versus ignition delay time plot for octane numbers ranging from 80 to 100. The data shown in Fig. 1a were fitted exponentially to obtain:

$$RON = 118.0867 - 139.5077 \times \exp\left(\frac{-IDT}{1.11278}\right) - 45.00948 \times \exp\left(\frac{-IDT}{6.2065}\right) - 19.7269 \times \exp\left(\frac{-IDT}{72.4718}\right) \quad (1)$$

R^2=0.9955

$$MON = -1298640 - 32.6186 \times \exp\left(\frac{-IDT}{12.6758}\right) - 109.4963 \times \exp\left(\frac{-IDT}{1.5107}\right) + 1298740 \times \exp\left(\frac{IDT}{19099100}\right) \quad (2)$$

R^2=0.9908

where IDT is the ignition delay time at 835 K and 20 atm in ms. The R^2 values are promising with the RON (R^2=0.9955) data having better fitting than the MON (R^2=0.9908) data.

3.2. Condition 2: Constant volume ignition delay times at 825 K and 25 atm

Next, ignition delay time for the various mixtures presented in Table 1 and Table S1 were calculated at the conditions (825 K, 25 atm) recommended by Mehl et al. [13]. Mehl et al. [13] proposed these conditions based on multiple ignition delay time calculations at various temperatures and pressures for many TPRF/1-hexene mixtures. They found that the AKI correlates reasonably well with ignition delay times at the proposed conditions. Figure 1b presents ignition delay times at 825 K and 25 atm (logarithmic scale) of the Kalghatgi et al. [22] and current TPRF mixtures versus the ON. The correlation between ignition delay times at 825 K and 25 atm and the ON is better than the correlation for the 835 K and 20 atm ignition delay times. For example, the three mixtures with similar RON (Table 2) have closer ignition delay times at 825 K and 25 atm, as illustrated in Table 2 (C2).

Octane numbers and ignition delay times at 825 K and 25 atm (Fig. 1b) were fitted according to the following exponential expressions,

$$RON = 116.4454 - 18.2418 \times exp\left(-\frac{IDT}{59.9858}\right) - 41.0467 \times exp\left(-\frac{IDT}{4.6849}\right) - 152.5195 \times exp\left(-\frac{IDT}{0.7556}\right) \quad (3)$$

R^2=0.998

$$MON = 526351.7 - 526253.5 \times exp\left(-\frac{IDT}{9200910}\right) - 28.35 \times exp\left(-\frac{IDT}{11.925}\right) - 106.15 \times exp\left(-\frac{IDT}{1.13}\right) \quad (4)$$

R^2=0.9874

The R^2 value (0.998) for RON is now higher due to less scatter in RON data (Fig. 1b) compared to Fig. 1a. However, the R^2 value (0.9874) for the MON correlation comes out to be lower than the previous correlation because of the larger scatter in the MON data in the range of 90 and above.

3.3. Condition 3: Constant volume ignition delay times at RON- and MON-like conditions

Knock in the CFR engine occurs when the pressure and temperature are near their maximum values. The in-cylinder pressure increases due to piston compression and flame front propagation. Mehl et al. [25] presented simulated in-cylinder temperature and pressure histories during RON and MON tests in the CFR engine. Figure 7 in [25] reveals that the in-cylinder pressure versus CAD (crank angle degree) is close under RON and MON conditions during the compression cycle. The pressure rise caused by flame propagation is higher at RON conditions compared to MON. The in-cylinder temperature history is always higher during MON test compared to RON due to the higher intake air temperature for MON test (ASTM D2770 standard) [30]. Also, Kalghatgi et al. [22] demonstrated that a significant contribution to the Livengood-Wu integral [1, 22] is actually in the last few crank angle degrees (CAD) before knock occurs. At engine speeds of 600 (RON) and 900 (MON) RPM, 15 ms corresponds to 54 CAD and 81 CAD for RON and MON conditions, respectively. Therefore, ignition delay times longer than 10 or 15 ms negligibly contribute to the Livengood-Wu integral [1, 22] and may not correlate well with the octane numbers. Consequently, the maximum pressure and temperature from the simulated RON and MON conditions that Mehl et al. [25] reported are tested here as RON- and MON-like conditions. As can be seen from Figure 7 in [25], RON has a maximum pressure of 50 atm and a maximum temperature of 850 K. similarly, MON has a maximum pressure of 45 atm and a maximum temperature of 980 K. The ignition delay times for the various mixtures presented in Table 1 and Table S1 were calculated at these conditions. Fig. 2 presents the RON and MON of the Kalghatgi et al. [22] and current TPRF mixtures versus the ignition delay times at RON- and MON-like conditions. As can be seen from Fig. 2, the correlation between ignition delay times and RON is better than what was observed with the two previous conditions. The three mixtures (Table 2) with similar RON values have closer ignition delay times of 9.45 ms, 9.11 ms and 8.81 ms, respectively. The MON correlation (Fig. 2) is more scattered than the previous conditions. The data in Fig. 2 was fitted using the equations below,

$$RON = 117.41654 - 17.99786 \times exp\left(-\frac{IDT}{22.0574}\right) - 41.40406 \times exp\left(-\frac{IDT}{1.7736}\right) - 184.6537 \times exp\left(-\frac{IDT}{0.30285}\right) \quad (5)$$

R^2=0.9989

$$MON = 119.8228 - 563.6194 \times exp\left(-\frac{IDT}{0.21002}\right) - 563.6174 \times exp\left(-\frac{IDT}{0.21004}\right) - 42.1142 \times exp\left(-\frac{IDT}{2.88312}\right) \quad (6)$$

R^2=0.9556

The R^2 of 0.9989 value for RON is the highest so far, however, the MON fitting R^2 (0.9556) is the lowest amongst the three tested conditions. It is noted that the binary mixtures of iso-octane and toluene are the ones causing much of the scatter in the high MON region. This might be due to some deficiency in the used chemical kinetic model for iso-octane and toluene at high temperatures and pressures.

3.4. Condition 4: Variable volume ignition delay times

The fuel/air mixtures inside the CFR engine experience a wide range of temperatures and pressures during the compression cycle. Also, the flame front generated by spark ignition causes the pressure and temperature of the end gas to further increase. Therefore, trying to correlate octane numbers from CFR engines with ignition delay times at constant volume conditions might not the best strategy. As mentioned earlier, Mehl et al. [25] presented simulated in-cylinder temperature and pressure histories during RON and MON tests in the CFR engine. To feed these temperature and pressure profiles into CHEMKIN PRO for ignition delay time calculations, the data presented in Fig. 7 of [25] was digitized. The pressure profiles are then converted into volume profiles using the isentropic relation. The calculated volume profiles are used as input in the CHEMKIN PRO simulations. The initial pressure and temperature values for the simulations are taken from the digitized simulation data; these are 1.05 atm / 330 K and 1.05 atm / 440 K for RON and MON conditions, respectively. These initial conditions correspond to the -160 CAD where the presented calculations start. The calculations presented in this work also start from -160 CAD in correspondence with the digitized data. The ignition delay times of the Kalghatgi et al. [22] and current TPRF mixtures were calculated using the digitized pressure/volume profiles. The same volume profile was fed for the calculation of ignition delay times of all the tested TPRF mixtures. Fig. 3 shows ON as a function of ignition delay times calculated using the variable volume profiles. As can be seen from Fig. 3, the scatter in the RON data is lower compared to the constant volume ignition delay times presented earlier (Figs. 1 and 2). Particularly, the three mixtures (Tables 2 and 3) with similar RON values have almost identical ignition delay times of 40.88 ms, 40.85 ms and 40.75 ms, respectively. Also, ignition delay times are now spanning a much smaller scale compared to the three constant volume cases. Here, ignition delay times are ranging from 39 ms to 49 ms for ON from 20 to 120. This causes the error in the predicted ON to be smaller. There is some scatter in the MON data between 70 and 80 ON but the rest of the curve is quite good.

Different fitting methods, including various exponential functions, were tested on the data presented in Fig. 3 and the fit that produced the highest R^2 values was a 4th order polynomial:

$$RON = (-0.071672 \times IDT^4) + (13.726733 \times IDT^3) - (914.559866 \times IDT^2) + (27056.926 \times IDT) - 299894.4872 \quad (7)$$

R^2=0.99824

$$MON = (-0.06139127 \times IDT^4) + (11.035927 \times IDT^3) - (742.4421207 \times IDT^2) + (22162.463827 \times IDT) - 247682.5414 \quad (8)$$

R^2=0.9917

More significant digits are needed because of the 4th order polynomial fit. The R^2 values for RON (0.99824) and MON (0.9917) fittings are slightly higher compared to the initial two constant volume cases considered in the previous section. However, the R^2 value of RON fitting for condition 3 is slightly higher than the one reported here.

Calculated ignition delay times for the four studied conditions for all mixtures of Table 1 and Table S1 are presented in Table S2 (Supplementary Material).

3.5. Comparisons between conditions 1-4

Using the correlations developed here, RON and MON were predicted for the TPRF mixtures from literature of Table 1 and compared with the measured values. Fig. 4 shows the predicted versus measured RON and MON values for the literature [4, 21, 29, 30] TPRF mixtures presented in Table 1 using the four correlations considered. As can be observed from Fig. 4, the best RON correlation with calculated ignition delay times is for condition 3 RON-like (850 K, 50 atm) where the R^2 value of the predicted versus measured RON fitting is 0.9983 and the worst correlation is for condition 1 (835 K, 20 atm) where R^2 is 0.9742. However, the highest R^2 value (0.9866) for MON correlation with simulated ignition delay times is for condition 1 (835 K, 20 atm) and the lowest R^2 (0.9556) is clearly for condition 3 MON-like (980 K, 45 atm) where the scatter was more observable in Fig. 2. The predicted RON and MON errors using the four different correlations are tabulated in Table 3 and Table 4, respectively. In addition, these predicted RON and MON errors from the different correlations are plotted in Fig. 5. Octane number errors are the differences between measurements and predictions. As can be seen from Fig. 5a, condition 3 (850 K and 50 atm, RON-like) produces RON errors that are relatively small (±1 RON) between the predicted and measured RON values for the various literature TPRF mixtures. The repeatability and reproducibility limits for RON measurements are about 0.2 and 0.7 RON [21], respectively. Therefore, any error in RON predictions that is less than ±0.7 RON is within the experimental uncertainty. Only 3 out of the 25 predictions have errors larger than ±0.7 RON using condition 3 RON-like. 15 out of 25 predictions have RON errors larger than ±0.7 RON using the correlation from condition 2. Conditions 1 and 4 are similar in terms of errors outside the uncertainty limits with 18 out of 25 for condition 4 and 17 out of 25 for condition 1. However, the RON errors from condition 4 are closer to the uncertainty limits compared to condition 1.

Errors in predicted MON are generally larger than RON errors. The repeatability and reproducibility limits for MON measurements are around 0.2 and 0.9 MON [21] and hence any error within ±0.9 MON is within the experimental uncertainty. As can be seen from Fig. 5b, condition 4 produces the lowest MON errors with 12 out

of 25 predictions have errors larger than ±0.9 MON. most of the predicted MON have errors outside the uncertainly limits using the other three conditions.

3.6. Condition 5: Compression ratio dependent ignition delay times

In a CFR engine, different fuels experience different pre-knocking pressure and temperature histories. This is caused by the different compression ratios (CR) required to make a certain fuel to knock. For example, a high octane number fuel requires the CFR engine to be operating at a high CR and a fuel with low octane number is tested at a relatively small CR. Therefore, the compression stroke and hence volume profile is compression ratio/ON dependent. In addition, the flame propagation effect is not same for all fuels. The pressure rise due to flame propagation depends on the adiabatic flame temperature and the flame speed of the tested fuel. Therefore, compression ratio dependent volume profiles which account for the piston compression stroke and flame effects need to be generated and used in ignition delay time simulations.

In the CFR engine, the compression ratio is changed by adjusting the cylinder head position which is monitored using digital counter readings (DCR). Often, the ON are tabulated for various DCR values, as stated in Tables A4.1 in ASTM D2699 [29] for RON and ASTM D2770 [30] for MON. The values in the tables are used for bracketing purposes using two primary reference fuel (PRF) mixtures. The DCR values are only used for simplification purposes; however, they are directly related to the compression ratio as per the following empirical correlation which is provided in the ASTM standards [33],

$$CR = \frac{6345}{1850 - Digital\ counter\ reading} + 1 \tag{9}$$

Having the compression ratio value, the clearance volume of the CFR engine is calculated using the following equation:

$$CR = \frac{V_{clearance} + V_{swept}}{V_{clearance}} \tag{10}$$

where the displacement (swept) volume of the standard CFR engine is 37.33 in^3 (bore=3.25”, stroke=4.5”). Those values are employed in the following equation to generate the compression ratio dependent compression stroke volume profiles:

$$Volume\ (t) = \pi . r^2 \left(R \sin\left(\frac{Engine\ Speed}{30\pi t}\right) + \sqrt{L^2 - R^2 \left(cos\left(\frac{Engine\ speed}{30\pi t}\right)\right)^2} \right) + V_{clearance} + \pi . r^2 (L + R) \tag{11}$$

where r is the piston radius which is equal to 1.625", R is the engine stroke divided by 2 and is equal to 2.25", and L is the rod length and it is equal to 10" [34]. The engine speed depends on the mode at which the CFR engine is operating, with speeds of 600 RPM and 900 RPM for RON and MON modes, respectively. This volume profile respects that the piston speed is zero at both the bottom dead centre (BDC) and top dead centre (TDC). The compression stroke was simulated in the ignition delay time calculations by feeding the generated volume profiles into CHEMKIN PRO. After the piston reaches the TDC, the reduction in pressure due to expansion and the increase in pressure due to flame propagation are combined. As described in Mehl et al. [25], the net effect of those two actions is a further pressure and temperature increase. Therefore, additional pressure and temperature increases were added as further volume reductions to the TDC volume. This additional volume reduction was calculated from the digitized pressure profiles from Mehl et al. [25] from TDC (CAD=0^{o}) to the start of pressure and temperature decays due to expansion because (CAD=10-15^{o}). The digitized pressure profiles for RON and MON conditions were converted into volume profiles using isentropic relations where the specific heat ratio is mixture dependent. The differences in volume profiles due to different specific heat ratios were negligible and hence the same volume reduction rate was added to the CR dependent compression stroke volume profiles. This implies that the volume reduction rate due to flame propagation is not mixture dependent and the same rate is utilized for all tested mixtures. This is considered as an acceptable assumption because the laminar flame speeds and the heat capacities of the examined mixtures are not too different. The volume profile calculations start from -160 CAD because the pressures and temperatures at that time are available from the calculations of Mehl et al. [25]. These pressures (1.05 atm for both RON and MON conditions) and temperatures (330 K for RON and 440 K for MON conditions) values were used as initial conditions for the ignition delay time simulations. To visualize the effect of varying octane numbers on the volume, pressure and temperature profiles, three TPRF mixtures with RON values of 63.7, 79 and 99.8 were chosen. Assuming that the CFR engine is running in RON mode, Fig. 6 shows the calculated volume profiles for the three different TPRF/air stoichiometric mixtures. As can be clearly seen from Fig. 6, the three mixtures have different volume profiles where the high RON mixture is subjected to smaller volumes because of the higher CR used when performing knock experiments. To further investigate the differences between the three mixtures, non-reacting (by setting the reaction rate multiplier to 0) CHEMKIN PRO simulations were run for the three TPRF/air stoichiometric mixtures using the presented volume profiles. Figure S1 and Figure S2 (Supplementary Material) show the pressure and temperature histories (logarithmic scale) from the non-reacting CHEMKIN PRO simulations. As can be observed from Fig. S1 and Fig. S2 (Supplementary Material), the higher RON mixtures experience higher pressures and temperatures throughout the entire compression cycle, particularly near the TDC. For simplicity and practicality, the excel sheets that are used to calculate the CR/ON dependent volume profiles for RON and MON conditions are provided in the Supplementary Material. The only needed input is the DCR value and the volume time histories are calculated according to equations 9-11.

Ignition delay times for all TPRF/air stoichiometric mixtures from the current study and Kalghatgi et al. [22] were calculated using the CR dependent volume profiles under RON and MON conditions. The calculated ignition delay times are presented in Table S2 in the Supplementary Material. Ignition delay times are plotted against the digital counter readings (DCR) in Fig. 7a for the TPRF mixtures under RON conditions. The DCR values were taken from [29] and [30] for RON and MON conditions, respectively. As can be observed from Fig. 7a, ignition delay time values for all TPRF mixtures are within 1 ms. Moreover, the ignition delay times have a very clear trend when plotted against DCR (or RON, as shown on the upper x-axis of Fig. 7a). The data points were fitted using a third-order polynomial:

$$IDT = -1.77 \times 10^{-8} \times DCR^3 + 3.53 \times 10^{-5} \times DCR^2 - 2.05 \times 10^{-2} \times DCR + 53.5, \quad R^2 = 0.9726 \tag{12}$$

Similarly, the ignition delay times under MON conditions are plotted against equivalent DCR in Fig. 7b. Again, the data were correlated very well and the difference between the fastest and slowest ignition delay times is 2 ms. The data points in Fig. 7b were fitted using a second-order polynomial.

$$IDT = -7.93 \times 10^{-6} \times DCR^2 + 1.14 \times 10^{-2} \times DCR + 28.7, \quad R^2 = 0.9104 \tag{13}$$

The ignition delay time correlation with DCR (or MON, as shown on the upper x-axis of Fig. 7b) has a lower R^2 value of 0.9104 compared to 0.9726 for the RON correlation. These R^2 values are lower than what was observed with the previous four conditions. However, the range at which the ignition delay times span using condition 5 (1 ms for RON and 2 ms for MON) are much narrower than what was shown earlier (200 ms for conditions 1 and 2, 100 ms for condition 3 and 10 ms for condition 4). The ignition delay time narrower range improves the accuracy of the prediction as will be shown in the next section.

Based on the correlation between ignition delay times and DCR, a new method for the prediction of ON is proposed. This methodology states that after curve-fitting the ignition delay times of various TPRF mixtures and their corresponding DCR, one can use this curve to predict the RON and MON of any TPRF mixture with known composition. The methodology can be used for ON as low as dictated by Tables A4.1 in [29, 30] and ON<100 because of the decreased accuracy in the measurements of RON values above 100 since the bracketing fuel (PRF) has octane ratings of 100 and less. All that is needed is providing CHEMKIN PRO with mole fractions of the TPRF mixture and a variable volume profile that corresponds to an estimated compression ratio. The initial variable volume profile is based on an estimated DCR. The resulting ignition delay time will be a point (A1) on one of the plots for RON (Fig. 7a) or MON (Fig. 7b). An illustration of the application of the method is presented in Fig. 8 for RON prediction. The next step depends on whether A1 is below or above the curve fit. In general, for a given TPRF mixture, ignition delay times decrease when increasing the digital counter reading. The DCR is increased by steps which become smaller (10 DCR) as the curve fit is approached to produce more points (A2, A3 and A4) and add them to the plot to generate the linear line drawn in Fig. 8. The calculations stop when the calculated line crosses the curve fit. The intersecting point is referred to as Ax in Fig.

8. The DCR for Ax is obtained from the plot and the corresponding predicted ON is looked up from Tables A4.1 from ASTM D2699 [29] for RON and ASTM D2770 [30] for MON. Another test case where the initial DCR guess results in a point below the curve is presented in Fig. 8.

In order to validate this method, the octane numbers of the literature TPRF mixtures given in Table 1 were predicted using the approach described here. The outcome is presented in Table 5, where the ON error is the difference between measurements and predictions. As can be seen from Table 5, the errors between the predicted and measured RON values for the various TPRF mixtures are relatively small (±1 RON). Only 6 out of the 20 predictions have errors more than ±0.7 RON. This is considered as a success of the developed prediction method for RON and it is comparable to the correlation using condition 3 RON-like. The errors in MON predictions are higher than those of RON. This is expected because of the larger scatter in the ignition delay times versus DCR data (Fig. 7b). Also, the larger difference between the minimum and maximum ignition delay times contributes to these larger errors. Therefore, 12 out of 21 predictions have larger errors than ±0.9 MON. It is noticed that the predictions with high errors are for the mixtures close to the maximum ignition delay times. The parabolic curve fit is peaking at that location which makes the intersection of calculation line and curve fit to be less precise and, hence, larger errors in the predictions occur there. The predictions using the proposed method were compared with the predictions using the linear-by-mole blending rule [21] and with the non-linear by mole method recently proposed by Kalghatgi et al. [22]. The comparisons between the predicted ON errors using the three methods are presented in Fig. 9 for RON and MON. As can be seen from Fig. 9a, the predicted RON error using the proposed method is comparable to the linear [21] and non-linear [22] by-mole blending rules where most of the RON errors are within the experimental uncertainty limits. Note that a significant limitation of the linear-by-mole blending rule is the assumption of the ON of toluene where the predicted ON errors are directly proportional to the ON of pure toluene which spans a range of almost 10 ON from various experimental measurements [21, 23]. Regarding MON, Fig. 9b shows that the linear and non-linear-by-mole do better job in predicting the MON for the tested TPRF mixtures than the proposed methodology and hence improvements for predicting MON are needed.

Prediction errors larger than the repeatability and reproducibility limits can be caused by one or more of the following:

- Deficiency in the prediction method, where ignition delay time is not the only chemical kinetic parameter that directly correlates with octane numbers.
- Deficiency in the compression ratio dependent volume profiles, where the flame propagation pressure and temperature rise are not modelled adequately and perhaps should be mixture dependent.
- Deficiency in the chemical kinetics model that is used for ignition delay time calculations. These ignition delay time calculations using the variable volume profiles form a very robust test for the chemical kinetic mechanism because the chemistry is tested at a very wide range of pressures (1-100

atm) and temperatures (330-1000 K) for TPRF mixtures of varying composition. The Lawrence Livermore national laboratory (LLNL) mechanism [13] used to perform the calculations in this work is known to work well for n-heptane as it has been validated over a wide range of n-heptane experiments. However, the iso-octane and toluene sub-mechanisms are not as mature, particularly at low to intermediate temperature ranges.

- Deficiency in the curve fitting due to limited experimental data.

4. Conclusions

This work examines potential relationship between octane numbers (RON and MON) and ignition delay times for binary and ternary toluene primary reference fuel (toluene/n-heptane/iso-octane) blends. Ignition delay times are calculated for:

- Four constant volume pairs:
  - Condition 1: 835 K, 20 atm
  - Condition 2: 825 K, 25 atm
  - Condition 3: 850 K, 50 atm (RON-like)
  - Condition 3: 980 K, 45 atm (MON-like)
- Condition 4: Variable volume profiles
- Condition 5: Compression ratio/octane number dependent variable volume profiles

Between the constant volume pairs, the 850 K and 50 atm conditions resulted in better correlation with the RON than the correlations from conditions 1, and 2. MON was best correlated with ignition delay times at condition 4 (variable volume) compared to conditions 1, 2 and 3. Finally, the compression ratio dependent volume profiles (condition 5) lead to better correlation with RON where most of the predicted RON values were within the repeatability and reproducibility limits of RON measurements in the CFR engine. Further work is needed to improve the prediction of MON using the proposed methodology.

Acknowledgments

This work has been supported by the Fuel Technology Division in Saudi Aramco R&DC. The work at King Abdullah University of Science and Technology (KAUST) is funded by KAUST and Saudi Aramco under the FUELCOM program.

Supplementary Material

The experimental ON measurements from literature are presented in Table S1. The calculated ignition delay times for various TPRF/air mixtures are provided in Tables S2-S3.

References

[1] G. Kalghatgi, Fuel/Engine Interactions, SAE International, Warrendale, PA, 2013.
[2] R. Stone, Introduction to Internal Combustion Engines, SAE International and Macmillan Press, New York, 2012.
[3] J.B. Heywood, Internal combustion engine fundamentals, Mcgraw-hill New York, 1988.
[4] N. Morgan, A. Smallbone, A. Bhave, M. Kraft, R. Cracknell, G. Kalghatgi, Mapping surrogate gasoline compositions into RON/MON space, Combustion and Flame, 157 (2010) 1122-1131.
[5] Annual book of ASTM standards, American Society for Testing & Materials, 2004.
[6] J.W. Hudgens, Workshop on Combustion Simulation Databases for Real Transportation Fuels, in, NIST, Gaithersburg, Maryland, 2003.
[7] W. Pitz, N. Cernansky, F.N. Dryer, F. Egolfopoulos, J.T. Farrell, D.G. Friend, H. Pitsch, Development of an experimental database and chemical kinetic models for surrogate gasoline fuels, SAE Technical Paper 2007-01-0175, (2007).
[8] G. Kalghatgi, Auto-ignition quality of practical fuels and implications for fuel requirements of future SI and HCCI engines, SAE Technical Paper 2005-01-0239, (2005).
[9] W.R. Leppard, The chemical origin of fuel octane sensitivity, SAE Technical Paper 90-21-37, (1990).
[10] B. Thirouard, J. Cherel, V. Knop, Investigation of mixture quality effect on CAI combustion, SAE Technical Paper 2005-01-0141, (2005).
[11] B.M. Gauthier, D.F. Davidson, R.K. Hanson, Shock tube determination of ignition delay times in full-blend and surrogate fuel mixtures, Combustion and Flame, 139 (2004) 300-311.
[12] J.C.G. Andrae, P. Björnbom, R.F. Cracknell, G.T. Kalghatgi, Autoignition of toluene reference fuels at high pressures modeled with detailed chemical kinetics, Combustion and Flame, 149 (2007) 2-24.
[13] M. Mehl, W.J. Pitz, C.K. Westbrook, H.J. Curran, Kinetic modeling of gasoline surrogate components and mixtures under engine conditions, Proceedings of the Combustion Institute, 33 (2011) 193-200.
[14] P.L. Perez, A.L. Boehman, Experimental Investigation of the Autoignition Behavior of Surrogate Gasoline Fuels in a Constant-Volume Combustion Bomb Apparatus and Its Relevance to HCCI Combustion, Energy & Fuels, 26 (2012) 6106-6117.
[15] C. Naik, W. Pitz, C. Westbrook, M. Sjöberg, J.E. Dec, J. Orme, H.J. Curran, J.M. Simmie, Detailed Chemical Kinetic Modeling of Surrogate Fuels for Gasoline and Application to an HCCI Engine, SAE Technical Paper 2005-01-3741, (2005).
[16] M. Fikri, J. Herzler, R. Starke, C. Schulz, P. Roth, G.T. Kalghatgi, Autoignition of gasoline surrogates mixtures at intermediate temperatures and high pressures, Combustion and Flame, 152 (2008) 276-281.
[17] M. Yahyaoui, N. Djebaïli-Chaumeix, P. Dagaut, C.E. Paillard, S. Gail, Experimental and modelling study of gasoline surrogate mixtures oxidation in jet stirred reactor and shock tube, Proceedings of the Combustion Institute, 31 (2007) 385-391.

[18] S.M. Sarathy, G. Kukkadapu, M. Mehl, W. Wang, T. Javed, S. Park, M.A. Oehlschlaeger, A. Farooq, W.J. Pitz, C.-J. Sung, Ignition of alkane-rich FACE gasoline fuels and their surrogate mixtures, Proceedings of the Combustion Institute, 35 (2015) 249-257.
[19] A. Ahmed, G. Goteng, V.S.B. Shankar, K. Al-Qurashi, W.L. Roberts, S.M. Sarathy, A computational methodology for formulating gasoline surrogate fuels with accurate physical and chemical kinetic properties, Fuel, 143 (2015) 290-300.
[20] J.C.G. Andrae, T. Brinck, G.T. Kalghatgi, HCCI experiments with toluene reference fuels modeled by a semidetailed chemical kinetic model, Combustion and Flame, 155 (2008) 696-712.
[21] V. Knop, M. Loos, C. Pera, N. Jeuland, A linear-by-mole blending rule for octane numbers of n-heptane/iso-octane/toluene mixtures, Fuel, 115 (2014) 666-673.
[22] G. Kalghatgi, H. Babiker, J. Badra, A Simple Method to Predict Knock Using Toluene, N-Heptane and Iso-Octane Blends (TPRF) as Gasoline Surrogates, SAR Paper, 2015-01-0757 (2015).
[23] T.M. Foong, K.J. Morganti, M.J. Brear, G. da Silva, Y. Yang, F.L. Dryer, The octane numbers of ethanol blended with gasoline and its surrogates, Fuel, 115 (2014) 727-739.
[24] H.J. Curran, P. Gaffuri, W.J. Pitz, C.K. Westbrook, W.R. Leppard, Autoignition chemistry in a motored engine: An experimental and kinetic modeling study, Symposium (International) on Combustion, 26 (1996) 2669-2677.
[25] M. Mehl, T. Faravelli, F. Giavazzi, E. Ranzi, P. Scorletti, A. Tardani, D. Terna, Detailed Chemistry Promotes Understanding of Octane Numbers and Gasoline Sensitivity, Energy & Fuels, 20 (2006) 2391-2398.
[26] M. Hori, H. Nakamura, T. Tezuka, S. Hasegawa, K. Maruta, Characteristics of n-heptane and toluene weak flames in a micro flow reactor with a controlled temperature profile, Proceedings of the Combustion Institute, 34 (2013) 3419-3426.
[27] M. Hori, A. Yamamoto, H. Nakamura, T. Tezuka, S. Hasegawa, K. Maruta, Study on octane number dependence of PRF/air weak flames at 1–5 atm in a micro flow reactor with a controlled temperature profile, Combustion and Flame, 159 (2012) 959-967.
[28] S.M. Sarathy, T. Javed, F. Karsenty, A. Heufer, W. Wang, S. Park, A. Elwardany, A. Farooq, C.K. Westbrook, W.J. Pitz, M.A. Oehlschlaeger, G. Dayma, H.J. Curran, P. Dagaut, A comprehensive combustion chemistry study of 2,5-dimethylhexane, Combustion and Flame, 161 (2014) 1444-1459.
[29] Standard test method for research octane number of spark-ignition engine fuel, ASTM D2699-08 (2008).
[30] Standard test method for motor octane number of spark-ignition engine fuel, ASTM D2700-08 (2008).
[31] Reaction Design, CHEMKIN-PRO, in, San Diego, 2011.
[32] M. Mehl, W.J. Pitz, C.K. Westbrook, K. Yasunaga, C. Conroy, H.J. Curran, Autoignition behavior of unsaturated hydrocarbons in the low and high temperature regions, Proceedings of the Combustion Institute, 33 (2011) 201-208.
[33] Standard test method for research octane number of spark-ignition engine fuel, ASTM D2699-61 (1961).
[34] D. Flowers, S. Aceves, R. Smith, J. Torres, J. Girard, R. Dibble, HCCI in a CFR Engine: Experiments and Detailed Kinetic Modeling, SAE Technical Paper 2000-01-0328, (2000).

Tables

Table 1. Experimental RON and MON data for TPRF mixtures.

n-heptane		Iso-octane		Toluene		RON	MON	S
(vol.%)	(mol.%)	(vol.%)	(mol.%)	(vol.%)	(mol.%)			
90.0	86.7	0.0	0.0	10.0	13.3	22.0	–	–
54.0	54.2	36.0	32.0	10.0	13.8	48.0	46.7	1.3
0.0	0.0	90.0	85.2	10.0	14.8	102.0	99.5	2.5
80.0	74.4	0.0	0.0	20.0	25.6	28	–	–
48.0	46.2	32.0	27.3	20.0	26.5	58	53.9	4.1
0.0	0.0	80.0	72.0	20.0	28.0	104.1	98.5	5.6
70.0	62.9	0.0	0.0	30.0	37.1	38	–	–
0.0	0.0	70.0	60.0	30.0	40.0	105.6	98.3	7.3
60.0	52.1	0.0	0.0	40.0	47.9	51.4	46	5.4
0.0	0.0	60.0	49.1	40.0	50.9	107.7	97	10.7
50.0	42.0	0.0	0.0	50.0	58.0	65.9	60.0	5.9
40.0	32.6	0.0	0.0	60.0	67.4	77	68.0	9
20.0	15.4	0.0	0.0	80.0	84.6	98.6	88.5	10.1

504 Table 2. Ignition delay times at 835 K and 20 atm for three different TPRF mixtures.

n-heptane		Iso-octane		Toluene		RON	MON	Ignition delay times (ms)	
(vol.%)	(mol.%)	(vol.%)	(mol.%)	(vol.%)	(mol.%)			C1	C2
36.0	36.9	54.0	49.0	10.0	14.1	66.0	64.4	3.81	2.45
42.0	38.8	28.0	22.9	30.0	38.2	66.1	61	3.40	2.30
50.0	42.0	0.0	0.0	50.0	58.0	65.9	60.0	3.06	2.15

505

506

507 Table 3. Predicted RON errors using the four correlations obtained from the condition 1-4.

n-heptane (mol.%)	Iso-octane (mol.%)	Toluene (mol.%)	Measured RON	Predicted RON Error			
				C1	C2	C3	C4
63.8	14.2	22	39	-0.35	0.16	0.43	0.21
42	0	58	65.9	2.99	1.72	1.05	0.92
34.4	0	65.6	75.6	2.53	1.17	0.24	-0.10
30.6	27.2	42.2	76.2	-0.04	0.18	0.28	0.01
27.2	0	72.8	85.2	3.00	1.87	0.83	1.22
17	69	14	85.7	-4.48	-2.29	-0.81	-0.27
17	63	20	86.6	-3.48	-1.61	-0.33	-0.65
16.9	59.9	23.3	87	-3.18	-1.48	-0.31	-1.07
23.7	0	76.3	89.3	2.71	1.68	0.74	1.59
20.8	0	79.2	92.3	1.98	0.99	0.20	1.49
15	35	50	93	0.03	0.28	0.47	-1.22
13.7	42.8	43.5	93	-0.91	-0.35	0.17	-2.21
20.3	0	79.7	93.4	2.43	1.44	0.69	2.04
10	65	25	93.7	-3.15	-1.78	-0.26	-4.55
9.8	56.5	33.7	95.2	-2.07	-1.15	-0.12	-3.65
12.3	34	53.7	96	-0.03	0.02	0.08	-1.18
13	27	60	96.3	0.39	0.18	-0.01	-0.51
16.5	3.5	80	96.9	1.73	0.88	0.28	1.88
16	0	84	97.7	1.14	0.31	-0.27	1.70
13.5	12	74.5	98	0.71	0.09	-0.48	0.72
12.6	7	80.4	99.8	0.62	0.03	-0.62	1.10
8.7	10.5	80.8	103.3	0.77	0.53	-0.36	1.00
4.8	14.1	81.1	107.6	2.34	2.28	1.02	1.62
0	39.2	60.8	110	4.02	4.07	1.65	1.77
0	18.4	81.6	113	4.33	4.04	0.18	1.92

508

509

Table 4. Predicted MON errors using the four correlations obtained from the condition 1-4.

n-heptane (mol.%)	Iso-octane (mol.%)	Toluene (mol.%)	Measured RON	Predicted RON Error			
				C1	C2	C3	C4
63.8	14.2	22	37	-3.05	-1.18	1.77	0.62
42	0	58	57.7	-2.57	-1.19	-1.76	-2.51
34.4	0	65.6	66.9	-2.87	-1.79	-3.64	-2.83
30.6	27.2	42.2	70.9	-1.83	0.65	1.19	0.74
27.2	0	72.8	74.8	-3.25	-2.16	-5.71	-1.84
17	69	14	84.6	0.22	4.06	4.80	6.33
17	63	20	84.2	-0.11	3.50	4.34	4.88
16.9	59.9	23.3	84	-0.38	3.11	3.96	3.99
23.7	0	76.3	78.2	-3.41	-2.08	-6.65	-1.51
20.8	0	79.2	80.7	-3.79	-2.16	-7.37	-1.68
15	35	50	85.8	-0.77	1.93	1.52	0.35
13.7	42.8	43.5	86.7	-0.63	2.38	2.56	0.33
20.3	0	79.7	81.5	-3.49	-1.82	-7.09	-1.36
10	65	25	90.3	0.41	4.34	5.74	1.01
9.8	56.5	33.7	90.5	0.21	3.81	5.04	0.62
12.3	34	53.7	88.3	-0.85	1.92	1.46	0.05
13	27	60	87.3	-1.74	0.81	-0.39	-0.59
16.5	3.5	80	85.2	-3.19	-1.21	-5.81	-1.00
16	0	84	86.2	-3.42	-1.42	-6.47	-0.92
13.5	12	74.5	87.4	-2.91	-0.71	-3.65	-0.94
12.6	7	80.4	88.7	-3.49	-1.37	-4.57	-1.03
8.7	10.5	80.8	92.6	-3.53	-1.42	-2.80	-0.76
4.8	14.1	81.1	96.6	-3.11	-1.05	-1.00	-0.69
0	39.2	60.8	99.3	-1.28	0.93	3.87	-0.51
0	18.4	81.6	100.8	-2.37	-0.16	-0.27	-2.36

513

514 Table 5. Predicted versus measured RON for TPRF mixtures from literature [4, 21, 29, 30].

n-heptane (mol.%)	Iso-octane (mol.%)	Toluene (mol.%)	Measured		Predicted		ON Error	
			RON	MON	RON	MON	RON	MON
42	0	58	65.9	57.7	62.8	57.5	-3.1	-0.2
34.4	0	65.6	75.6	66.9	74.7	67.2	-0.9	0.3
30.6	27.2	42.2	76.2	70.9	76.1	67.4	-0.1	-3.5
27.2	0	72.8	85.2	74.8	83.9	77.5	-1.3	2.6
17	69	14	85.7	84.6	85.1	80.2	-0.6	-4.4
17	63	20	86.6	84.2	86.3	81.9	-0.3	-2.3
16.9	59.9	23.3	87	84	86.5	82.9	-0.5	-1.1
23.7	0	76.3	89.3	78.2	89	81.4	-0.3	3.2
20.8	0	79.2	92.3	80.7	92	84.1	-0.3	3.4
15	35	50	93	85.8	93.9	85.8	0.9	0
13.7	42.8	43.5	93	86.7	94	86.5	1	-0.2
20.3	0	79.7	93.4	81.5	92.9	84.5	-0.5	3
10	65	25	93.7	90.3	94.3	88.6	0.6	-1.7
9.8	56.5	33.7	95.2	90.5	96.5	88.6	1.3	-1.9
12.3	34	53.7	96.3	87.3	96.8	87.2	0.5	-0.1
13	27	60	96.3	88.3	96.9	87.3	0.6	-1
16.5	3.5	80	96.9	85.2	96.4	86.7	-0.5	1.5
16	0	84	97.7	86.2	97	87.6	-0.7	1.4
13.5	12	74.5	98	87.4	98.2	87.9	0.2	0.5
12.6	7	80.4	99.8	88.7	99.2	89.2	-0.6	0.5
8.7	10.5	80.8	103.3	92.6	---	92.6	---	0

515

516

Figure Captions

Fig. 1. Calculated ignition delay times (logarithmic scale) at a) 835 K and 20 atm and b) 825 K and 25 atm for stoichiometric TPRF/air mixtures versus ON.

Fig. 2. Calculated ignition delay times (logarithmic scale) at 850 K and 50 atm (RON-like) and 980 K and 45 atm (MON-like) for stoichiometric TPRF/air mixtures versus RON.

Fig. 3. Calculated ignition delay times using variable volume profiles for stoichiometric TPRF/air mixtures versus ON.

Fig. 4. Calculated versus measured RON and MON using ignition delay times at the four studied conditions C1-C4.

Fig. 5. Comparison of predicted a) RON error and b) MON error using the four different correlations using conditions C1-C4.

Fig. 6. Calculated volume profiles for three TPRF mixtures with different RON values.

Fig. 7. Ignition delay times using CR dependent volume profiles for the TPRF/air mixtures from the current study and Kalghatgi et al. [22] at a) RON conditions and b) MON conditions.

Fig. 8. An illustration of applying the new method to predict the ON for a given TPRF mixture.

Fig. 9. Comparison of predicted a) RON error and b) MON error using three different methods.

Figures

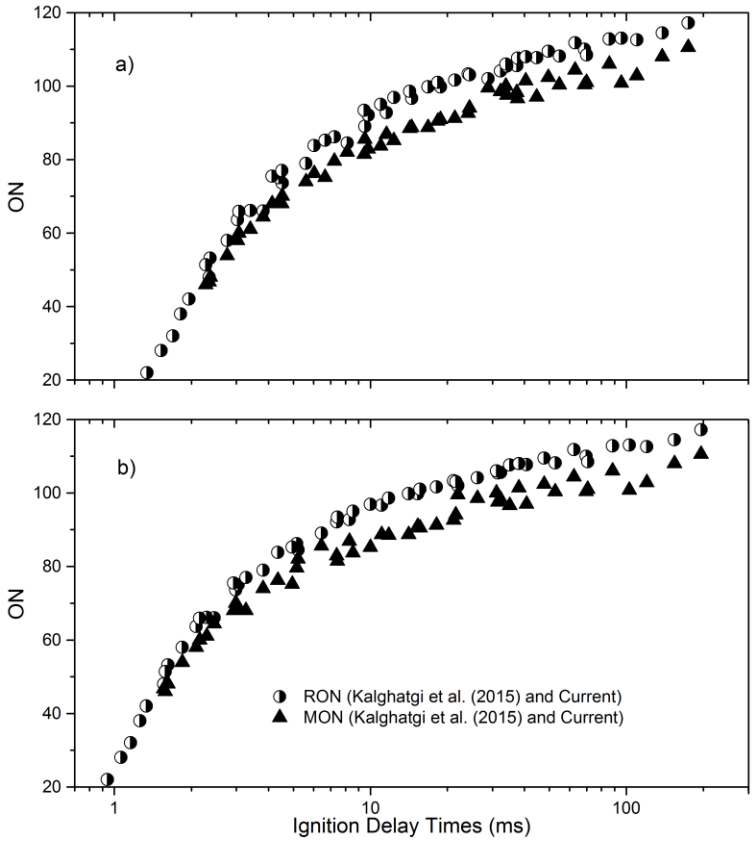

Fig. 1. Calculated ignition delay times (logarithmic scale) at a) 835 K and 20 atm and b) 825 K and 25 atm for stoichiometric TPRF/air mixtures versus ON.

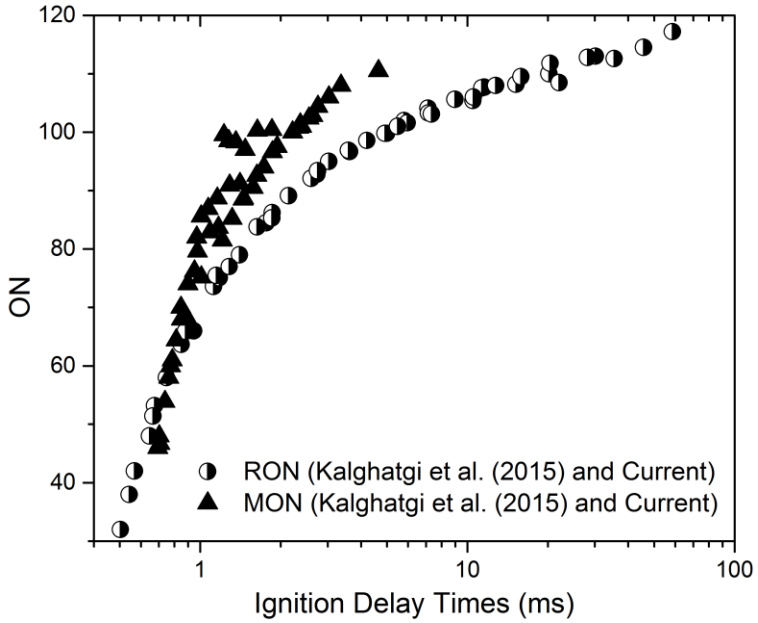

538

539 Fig. 2. Calculated ignition delay times (logarithmic scale) at 850 K and 50 atm (RON-like) and 980 K and 45
540 atm (MON-like) for stoichiometric TPRF/air mixtures versus RON.

541

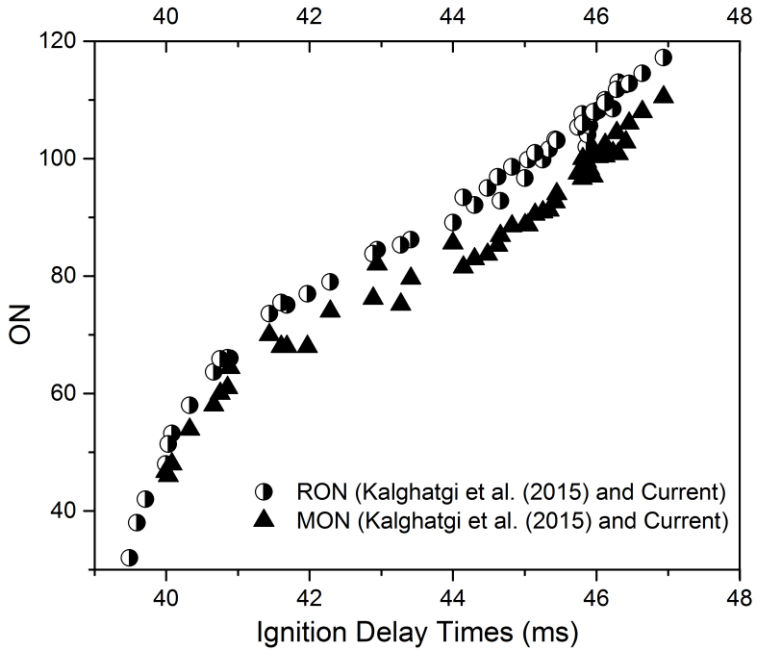

542

543 Fig. 3. Calculated ignition delay times using variable volume profiles for stoichiometric TPRF/air mixtures
544 versus ON.

545

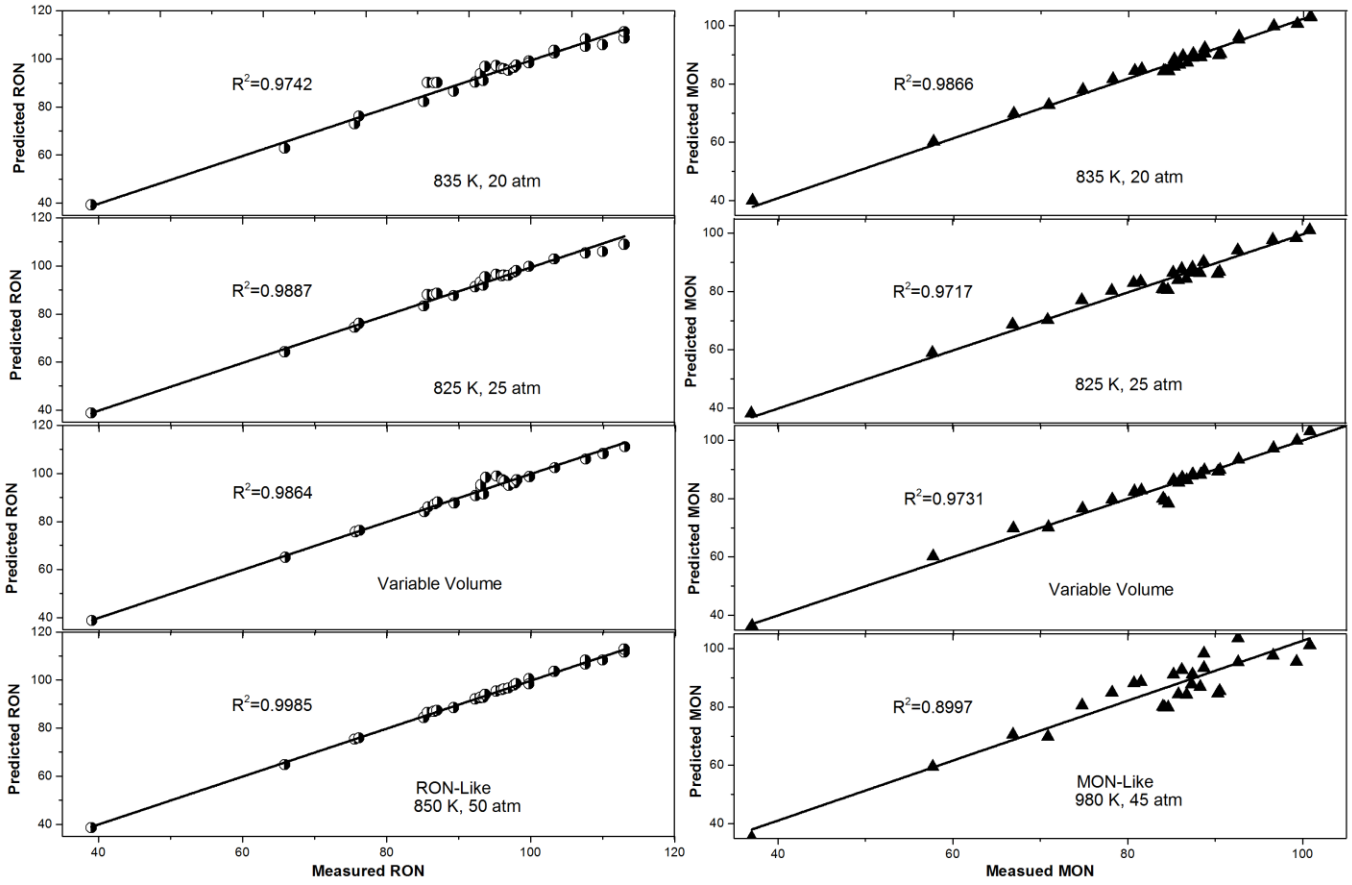

546

547 Fig. 4. Calculated versus measured RON and MON using ignition delay times at the four studied conditions C1-
548 C4.

549

550

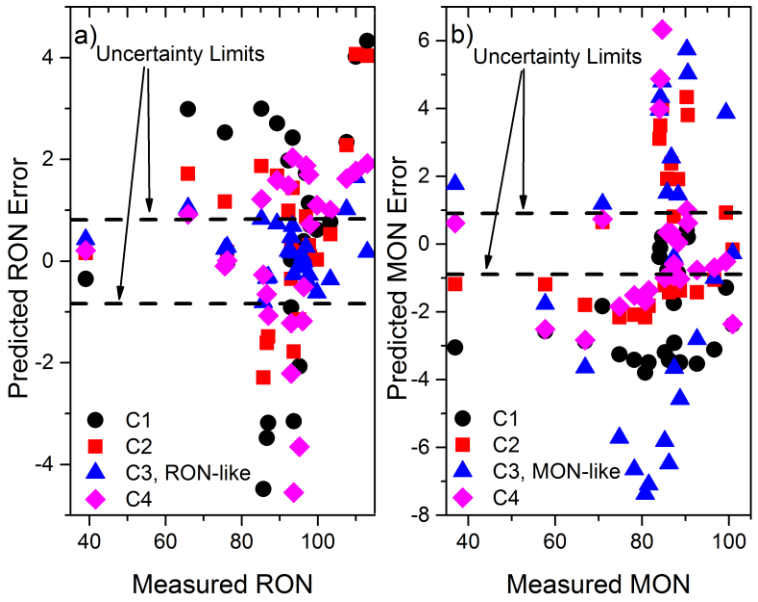

551

552 Fig. 5. Comparison of predicted a) RON error and b) MON error using the four different correlations using
553 conditions C1-C4.

554

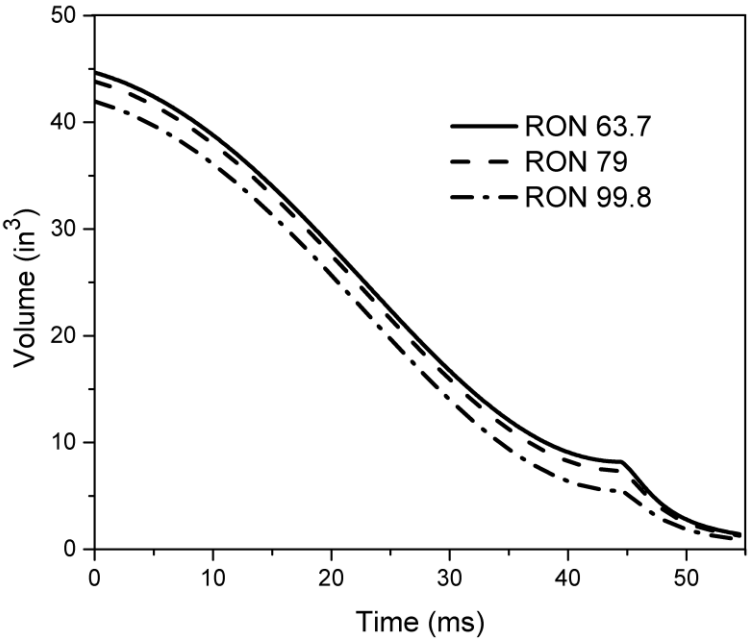

555

556 Fig. 6. Calculated volume profiles for three TPRF mixtures with different RON values.

557

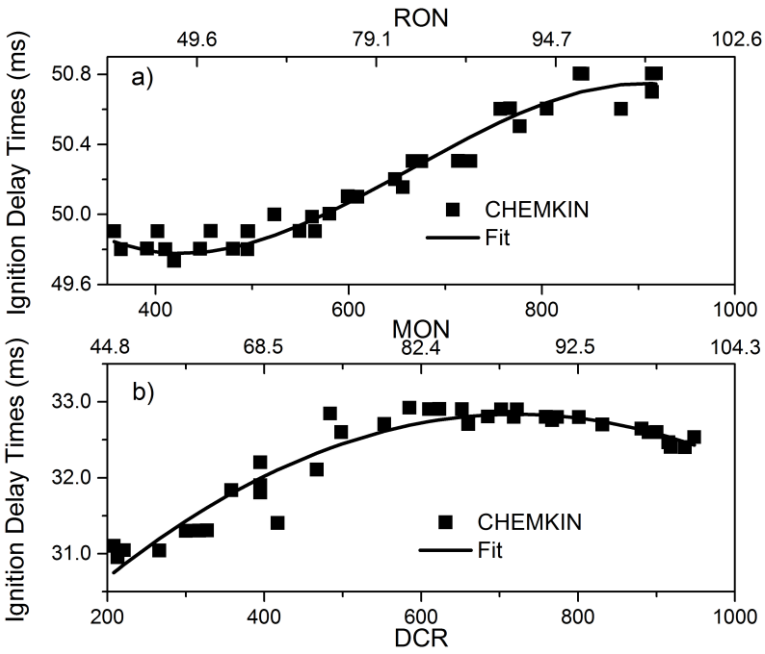

558

559 Fig. 7. Ignition delay times using CR dependent volume profiles for the TPRF/air mixtures from the current
560 study and Kalghatgi et al. [22] at a) RON conditions and b) MON conditions.

561

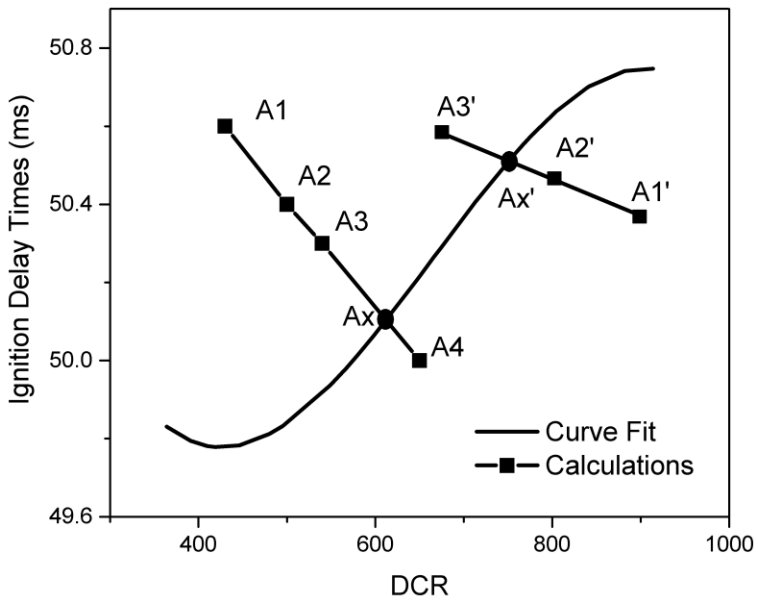

562

563 Fig. 8. An illustration of applying the new method to predict the ON for a given TPRF mixture.

564

565

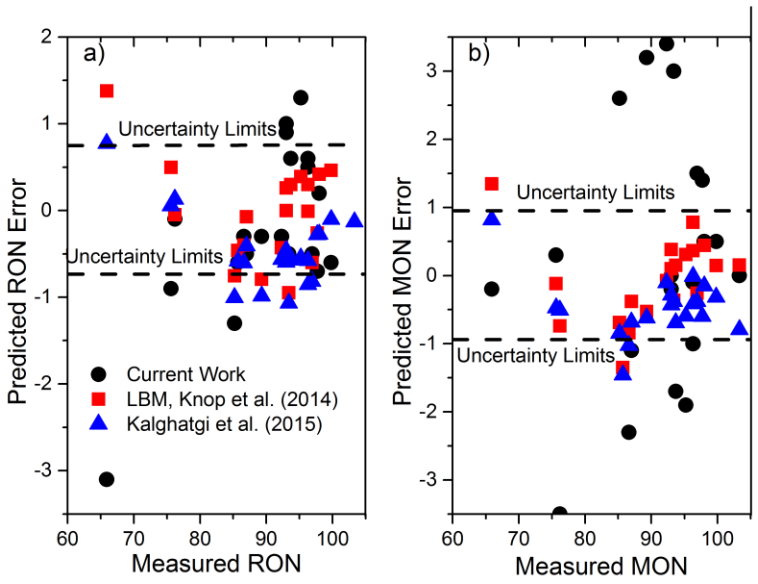

566

567 Fig. 9. Comparison of predicted a) RON error and b) MON error using three different methods.